

MENI

1993 Mendocino Triple Junction Experiment

Submitted By

N. Godfrey, B. Beaudoin, C. Lendl, A. Meltzer, J. Luetgert
Stanford University, Stanford, CA 94305
Oregon State University, Corvallis, OR 97331
Lehigh University, Bethlehem, PA 18015
US Geological Survey, Menlo Park, CA 94025

PASSCAL Data Report 96-018



Distributed by

*Incorporated Research Institutions for Seismology
Data Management Center
1408 NE 45th Street
Suite 201
Seattle, Washington 98105*

CONTENTS

1 Introduction.....	1
2 Geologic setting.....	1
3 Data acquisition.....	1
4 Instruments.....	5
5 Comparison of instrument responses of collocated instruments.....	7
6 Data reduction.....	18
7 Record sections.....	19
8. Multichannel reflection lines	54
Acknowledgments.....	63
References.....	63

FIGURES

Figure 1 Map showing the location of the wide-angle reflection/refraction lines.....	2
Figure 2a Station elevations for Line 1.....	3
Figure 2b Station elevations for Line 6.....	4
Figure 2c Station elevations for Line 9.....	4
Figure 4 SGR response.....	5
Figure 5 REFTEK response.....	6
Figure 6 PRS response.....	6
Figure 7a Traces from collocated station 6208 for shotpoint 603.....	8
Figure 7b Spectra from collocated station 6208 for shotpoint 603.....	9
Figure 8a Traces from collocated station 6208 for shotpoint 604.....	10
Figure 8b Spectra from collocated station 6208 for shotpoint 604.....	11
Figure 9a Traces from collocated station 1208 for shotpoint 101.....	12
Figure 9b Spectra from collocated station 1208 for shotpoint 101.....	13
Figure 10a Traces from collocated station 6208 for shotpoint 608.....	14
Figure 10b Spectra from collocated station 6208 for shotpoint 608.....	15
Figure 11a Traces from collocated station 6208 for shotpoint 606.....	16
Figure 11b Spectra from collocated station 6208 for shotpoint 606.....	17
Figure 12 Shot gather for shotpoint 101 (vertical component, reduced at 6 km/s).....	21
Figure 13 Shot gather for shotpoint 102 (vertical component, reduced at 6 km/s).....	22
Figure 14 Shot gather for shotpoint 103 (vertical	

component, reduced at 6 km/s).....	23
Figure 15 Shot gather for shotpoint 104 (vertical component, reduced at 6 km/s).....	24
Figure 16 Shot gather for shotpoint 105 (vertical component, reduced at 6 km/s).....	25
Figure 17 Shot gather for shotpoint 106 (vertical component, reduced at 6 km/s).....	26
Figure 18 Shot gather for shotpoint 107 (vertical component, reduced at 6 km/s).....	27
Figure 19 Shot gather for shotpoint 108 (vertical component, reduced at 6 km/s).....	28
Figure 20 Shot gather for shotpoint 601 (vertical component, reduced at 6 km/s).....	29
Figure 21 Shot gather for shotpoint 602 (vertical component, reduced at 6 km/s).....	30
Figure 22 Shot gather for shotpoint 603 (vertical component, reduced at 6 km/s).....	31
Figure 23 Shot gather for shotpoint 604 (vertical component, reduced at 6 km/s).....	32
Figure 24 Shot gather for shotpoint 605 (vertical component, reduced at 6 km/s).....	33
Figure 25 Shot gather for shotpoint 606 (vertical component, reduced at 6 km/s).....	34
Figure 26 Shot gather for shotpoint 607 (vertical component, reduced at 6 km/s).....	35
Figure 27 Shot gather for shotpoint 608 (vertical component, reduced at 6 km/s).....	36
Figure 28 Shot gather for shotpoint 901 (vertical component, reduced at 6 km/s).....	37
Figure 29 Shot gather for shotpoint 902 (vertical component, reduced at 6 km/s).....	38
Figure 30 Shot gather for shotpoint 903 (vertical component, reduced at 6 km/s).....	39
Figure 31 Shot gather for shotpoint 904 (vertical component, reduced at 6 km/s).....	40
Figure 32 Shot gather for shotpoint 905 (vertical component, reduced at 6 km/s).....	41
Figure 33 Shot gather for shotpoint 906 (vertical component, reduced at 6 km/s).....	42
Figure 34 Shot gather for shotpoint 907 (vertical component, reduced at 6 km/s).....	43
Figure 35 Shot gather for shotpoint 908 (vertical component, reduced at 6 km/s).....	44
Figure 36 Shot gather for shotpoint 909 (vertical component, reduced at 6 km/s).....	45
Figure 37 Shot gather for shotpoint 910 (vertical component, reduced at 6 km/s).....	46
Figure 38 Shot gather for shotpoint 911 (vertical component, reduced at 6 km/s).....	47

Figure 39 Shot gather for shotpoint 104 (horizontal north-south component, reduced at 3.46 km/s).....	48
Figure 40 Shot gather for shotpoint 104 (horizontal east-west component, reduced at 3.46 km/s).....	49
Figure 41 Shot gather for shotpoint 605 (horizontal north-south component, reduced at 3.46 km/s).....	50
Figure 42 Shot gather for shotpoint 605 (horizontal east-west component, reduced at 3.46 km/s).....	51
Figure 43 Shot gather for shotpoint 906 (horizontal north-south component, reduced at 3.46 km/s).....	52
Figure 44 Shot gather for shotpoint 906 (horizontal east-west component, reduced at 3.46 km/s).....	53
Figure 45 Map showing the location of the Bison reflection spread.....	55
Figure 46 Shotgather for shotpoint 101 recorded by the Bison reflection array.....	56
Figure 47 Shotgather for shotpoint 102 recorded by the Bison reflection array.....	56
Figure 48 Shotgather for shotpoint 103 recorded by the Bison reflection array.....	56
Figure 49 Shotgather for shotpoint 104 recorded by the Bison reflection array.....	56
Figure 50 Shotgather for shotpoint 105 recorded by the Bison reflection array.....	56
Figure 51 Shotgather for shotpoint 106 recorded by the Bison reflection array.....	57
Figure 52 Shotgather for shotpoint 107 recorded by the Bison reflection array.....	57
Figure 53 Shotgather for shotpoint 108 recorded by the Bison reflection array.....	57
Figure 54 Shotgather for shotpoint 902 recorded by the Bison reflection array.....	57
Figure 55 Shotgather for shotpoint 903 recorded by the Bison reflection array.....	57
Figure 56 Shotgather for shotpoint 904 recorded by the Bison reflection array.....	58
Figure 57 Shotgather for shotpoint 905 recorded by the Bison reflection array.....	58
Figure 58 Shotgather for shotpoint 907 recorded by the Bison reflection array.....	58
Figure 59 Shotgather for shotpoint 107 recorded by the Bison reflection array.....	58
Figure 60 Amplitude and Frequency spectra for trace 4 from shot 106.....	59
Figure 61 Amplitude and Frequency spectra for trace 20 from shot 106.....	60
Figure 62 Amplitude and Frequency spectra for trace 25 from shot 106.....	61
Figure 63 Amplitude and Frequency spectra for	

trace 30 from shot 106.....	62
-----------------------------	----

TABLES

Table 1 Shotpoint Locations and shot sizes for the shotpoints from Lines 1, 6 and 9.....	64
Table 2 Station locations, elevations and instrument type for the stations on Line 1.....	65
Table 3 Station locations, elevations and instrument type for the stations on Line 6.....	71
Table 4 Station locations, elevations and instrument type for the stations on Line 9.....	77
Table 5 SEG Y header values.....	82
Table 6 Positions and channel numbers of collocated instruments.....	82
Table 7 Positions and channel numbers of instruments at shotpoints.....	82
Table 8 Summary of the shots recorded by the Bison reflection spread at Lake Pillsbury.....	83

1) INTRODUCTION

In August 1993 the USGS, Stanford University, Lehigh University, Oregon State University and Rice University collaborated to record three onshore seismic lines with a total length of 650 km in the Mendocino Triple Junction Region. These three lines are part of an on-going seismic study designed to investigate the interactions of the Pacific Plate, the North American Plate and the Juan de Fuca/Gorda Plate in the Triple Junction region where the three plates meet. The onshore lines shot in 1993, Lines 1, 6 and 9, and the locations of the shots and receivers are shown in Figure 1. The shots were detonated in drill holes that had depths ranging from 30 m to 60 m.

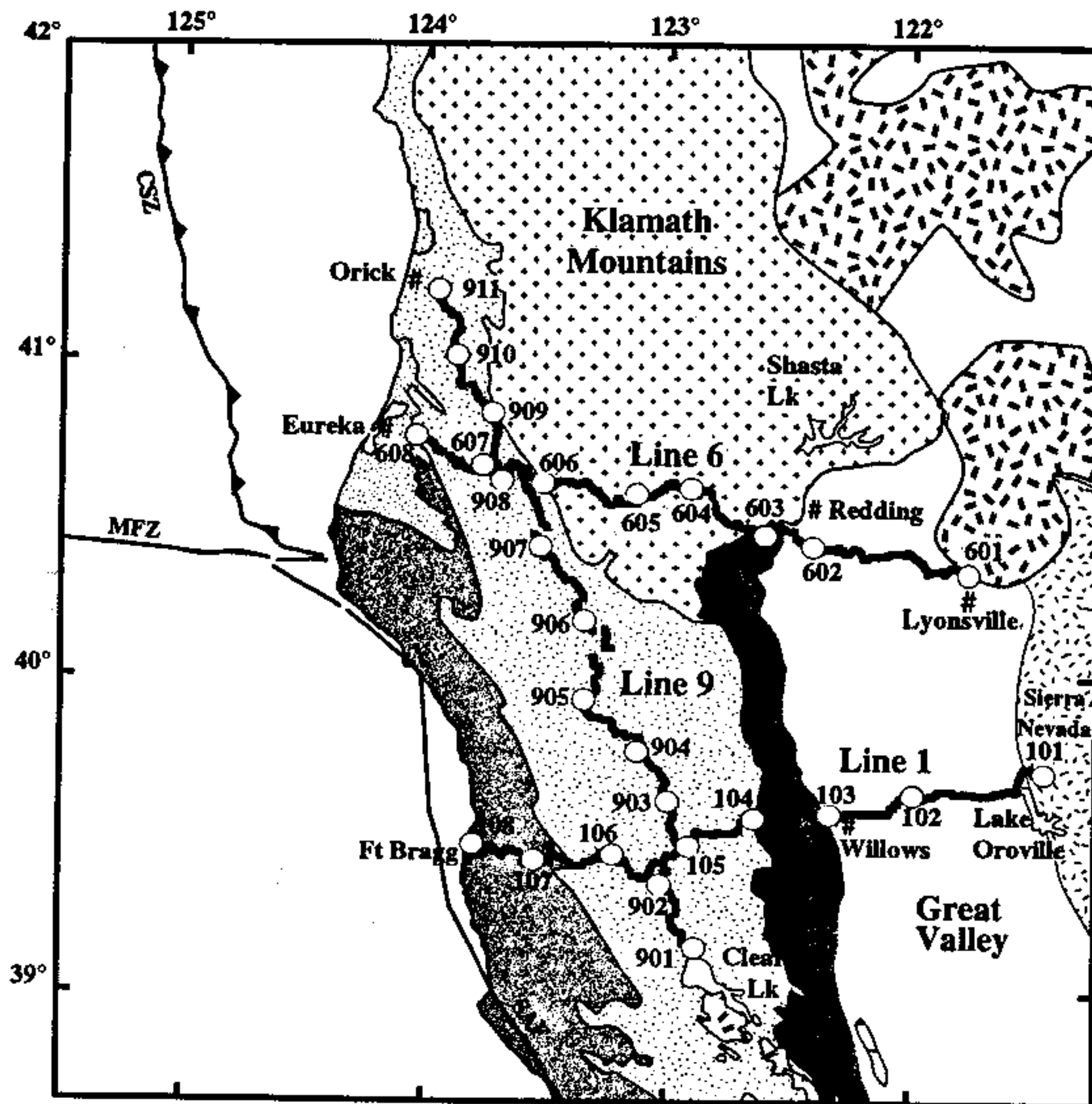
2) GEOLOGIC SETTING

The Mendocino Triple Junction marks the point where three plates, the North American, the Pacific and the Gorda, meet and interact. The San Andreas Fault Zone is the boundary between the Pacific plate and North American plate, the Cascadia Subduction Zone is the boundary between the North American plate and the Gorda plate and the Mendocino Fracture Zone is the boundary between the Gorda plate and the Pacific plate. The Gorda plate is currently being subducted beneath the North American plate north of the Mendocino Triple Junction, whilst the Pacific plate and North American plates are sliding past one another along a transform margin (the San Andreas Fault Zone) south of the Mendocino Triple Junction.

The Mendocino Triple Junction has been migrating north since its inception 25 - 30 million years ago, and as a result, the transform margin has lengthened to the north as subduction shuts down. It has been proposed that as the subducting slab 'retreats' northwards, a slabless window is left in its wake (Dickinson and Snyder, 1979). Jachens and Griscom (1983) have proposed that the southern edge of the presently subducting Gorda slab runs in an north west-south east direction from the triple junction to at least the Great Valley. Smith et al (1993) believe that the southern edge of the Gorda Plate runs in an east-west direction as a direct extension of the Mendocino Fracture Zone. Line 1 samples the current transform regime and aims to provide information about how the lithosphere responds to a change from a subduction environment to a transform environment. Line 6 samples the subduction regime and aims to provide information about the current subduction zone. Line 9 crosses the transition from subduction in the north to transform motion in the south and aims to provide information about how the transition is accommodated in the lithosphere, and where the edge of the currently subducting Gorda slab is.

3) DATA ACQUISITION

Station locations were determined by drawing a straight line on a map from the first shotpoint on the line to the last shotpoint on the line, marking points every 350 m (for east - west lines) or 400 m (for the north - south line) along this line,



Legend







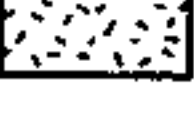
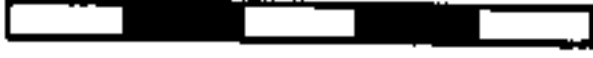


-  Miocene and younger sediments
 -  King Range and Coastal Belt Franciscan
 -  Central and Eastern Belt Franciscan
 -  Klamath Mountain Terrane
 -  Mesozoic Great Valley
 -  Tertiary Volcanics
 -  Sierra Nevada Batholith
- 
 100 km
 shotpoint
 thrust fault (teeth on upper plate)

Figure 1: map of northern California showing the shotpoints (open circles) and station locations (solid lines) for the Mendocino Triple Junction Experiment.

and then projecting these points perpendicularly from the line to the closest accessible rural road, National Forest road or logging road. Prior to the experiment, the shotpoint locations and station locations marked on the 1:24,000 maps (USGS 7.5 minutes series) were surveyed using the Global Positioning System (GPS) referenced to the WGS-84 reference system. Surveying crews completed this task between March and July of 1993. The GPS data at each station location was reduced relative to a base station operated by Trimble Navigation in Sunnyvale, California. For various reasons, including not being able to receive the minimum of four satellites for a 3D fix and not being able to read some of the base station data to allow data reduction, many of the locations had to be digitized from the 1:24,000 maps. The information on how the location data was obtained is recorded in Tables 1 through 4. The accuracy of positioning using GPS is 5 m for horizontal positions and 10 m for vertical positions. The accuracy of positioning by digitizing is about 25 m for horizontal positions and about 10 m for vertical positions, although this is strongly dependent on the distribution of contours and the contour interval.

To avoid cultural noise, seismographs were mainly deployed on rural roads and private land such as National Forest roads and logging roads, and the shots were fired at night, between midnight and 4:00 am.

Line 1 is a 200-km-long east-west line that runs from Lake Oroville to Ft. Bragg consisting of data from 571 seismographs and eight shot points. The shots were nominally 25 km apart (except shotpoints 101 and 102 which are about 45 km apart) and ranged in size from 400 - 2000 kg. Exact locations of the shots and the size of the shots can be found in Table 1. The seismographs were nominally 350 m apart and exact locations of the instruments can be found in Table 2. Shot and station locations are shown in Figure 1. Station elevations ranged from 20 m above sea-level to 1665 m above sea level and are shown in Figure 2a.

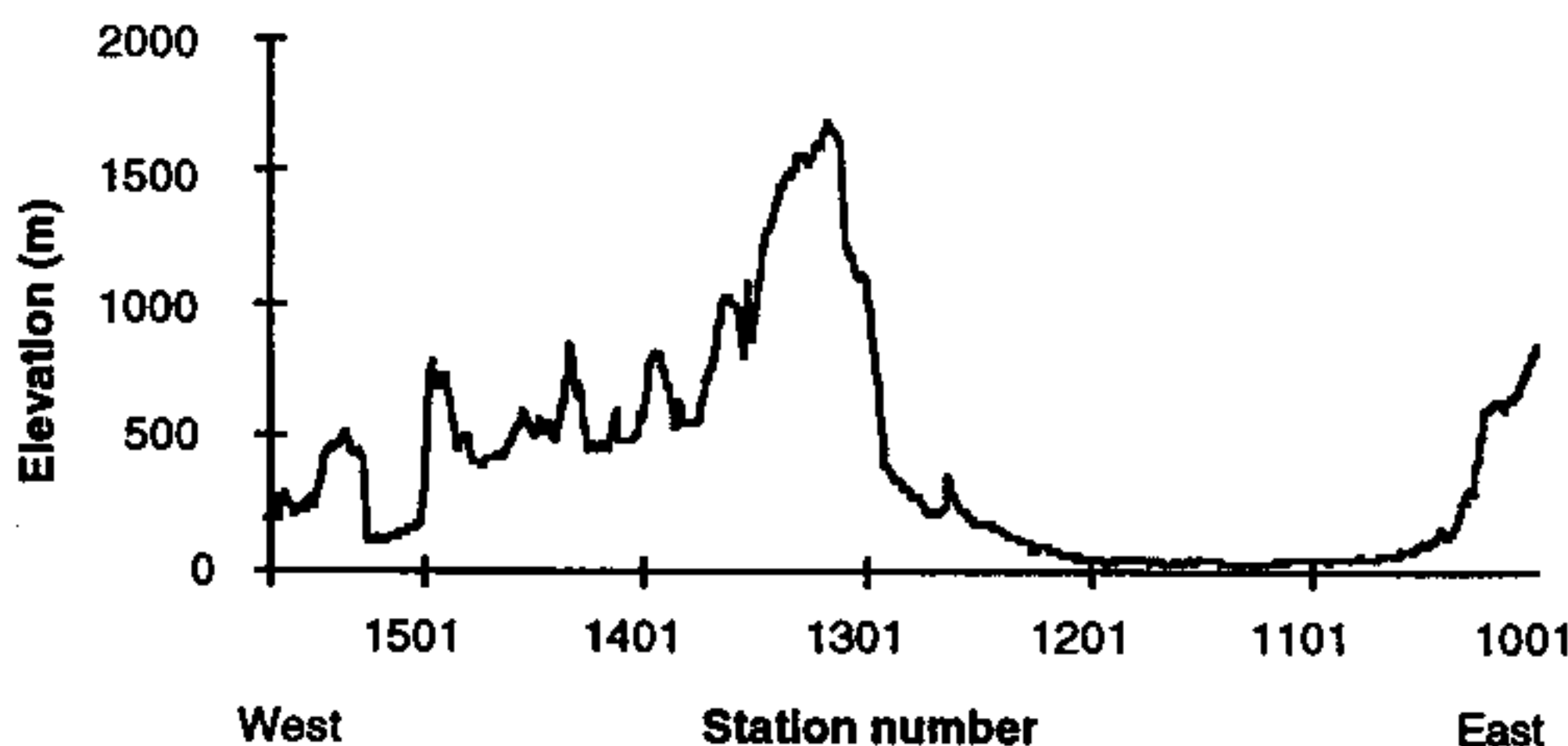


Figure 2a: station elevations for Line 1

Line 6 is a 200-km-long east-west line that runs from Lyonsville to Eureka consisting of data from 566 seismographs and eight shot points. The shots were nominally 25 km apart except for shotpoints 601 and 602 which were about 55 km apart) and ranged in size from 400 - 2000 kg. Exact locations of the shots and

the size of the shots can be found in Table 1. The seismographs were nominally 350 m apart and exact locations of the instruments can be found in Table 3. Shot and station locations are shown in Figure 1. Station elevations range from 111 m above sea-level to 1669 m above sea-level and are shown in Figure 2b.

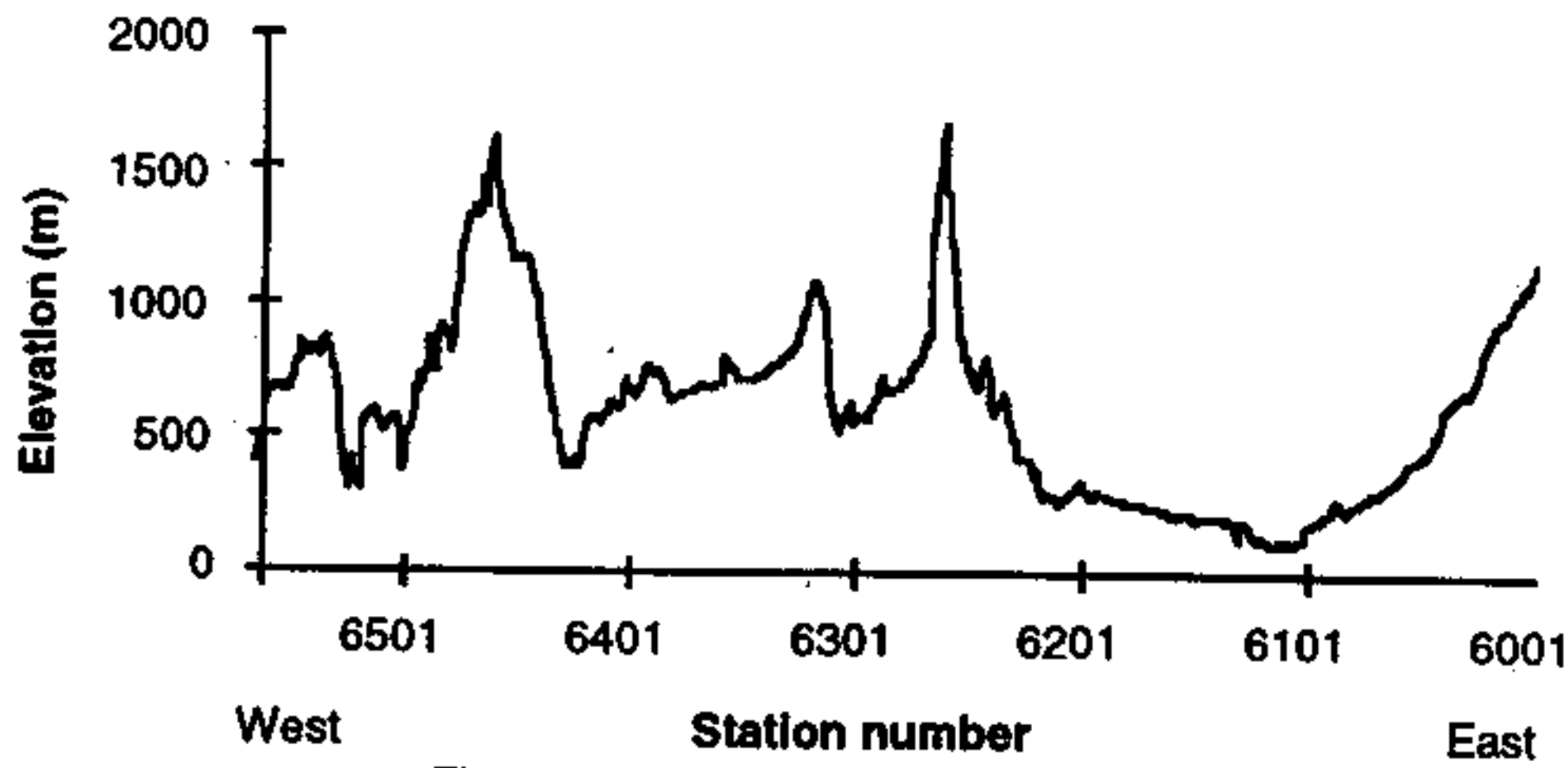


Figure 2b: station elevations for line 6

Line 9 is a 250-km-long north west-south east line that runs from Orick to Clear Lake consisting of data from 556 seismographs and eleven shot points. The shots were nominally 25 km apart and ranged in size from 400 - 2000 kg. Exact locations of the shots and the size of the shots can be found in Table 1. The seismographs were nominally 400 m apart and exact locations of the instruments can be found in Table 4. Shot and station locations are shown in Figure 1. Station elevations ranged from 162 m above sea-level to 1976 m above sea-level and are shown in Figure 2c.

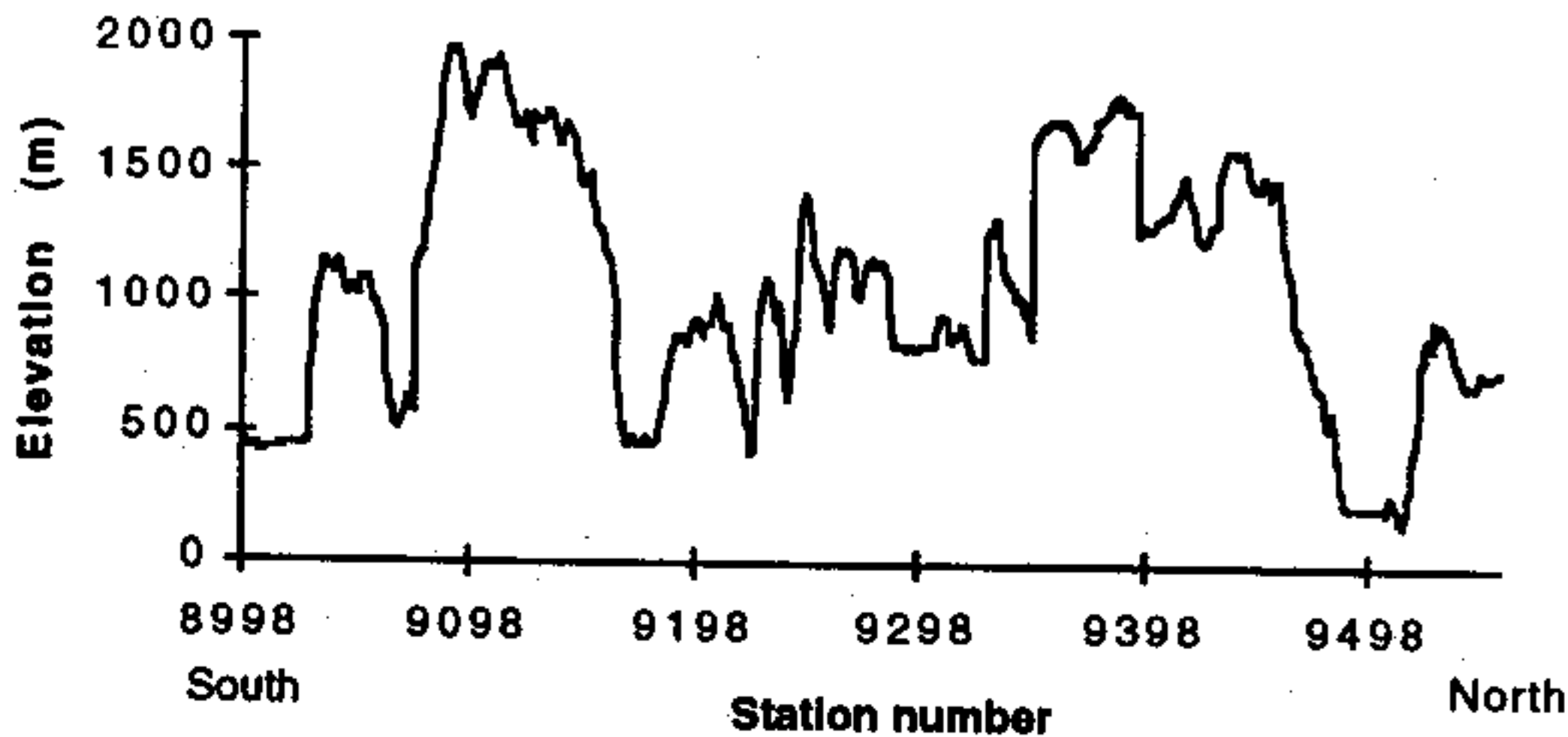


Figure 2c: station elevations for line 9

The three component instruments (REFTEKS and PRS-4s) were deployed with the horizontal components of the geophones oriented north-south and east-west (with respect to magnetic north).

4) INSTRUMENTS

Three different types of seismograph were used in the experiment: 180 Seismic Group Recorders (SGRs) which are owned by Stanford University, 165 REFTEKS operated by IRIS/PASCALL and 220 Portable Refraction Seismographs (PRS's) (185 PRS-1s and 35 PRS-4s) which are operated by the Geological Survey of Canada (GSC).

SGR

The SGRs were designed by Amoco Production Company, built by Globe Universal Sciences Inc. and have been modified by the USGS to turn on at preset times rather than by radio trigger. They are single channel, digital instruments with a theoretical range of 156 dB that record onto cassette tapes. They record at a sample rate of 4 ms and were connected to either single strings of 6 Marks Products L-10B vertical component 8 Hz geophones connected in series or to single Marks Products L4A 2 Hz geophones. Their response function is shown in Figure 4 (Murphy et al, 1992).

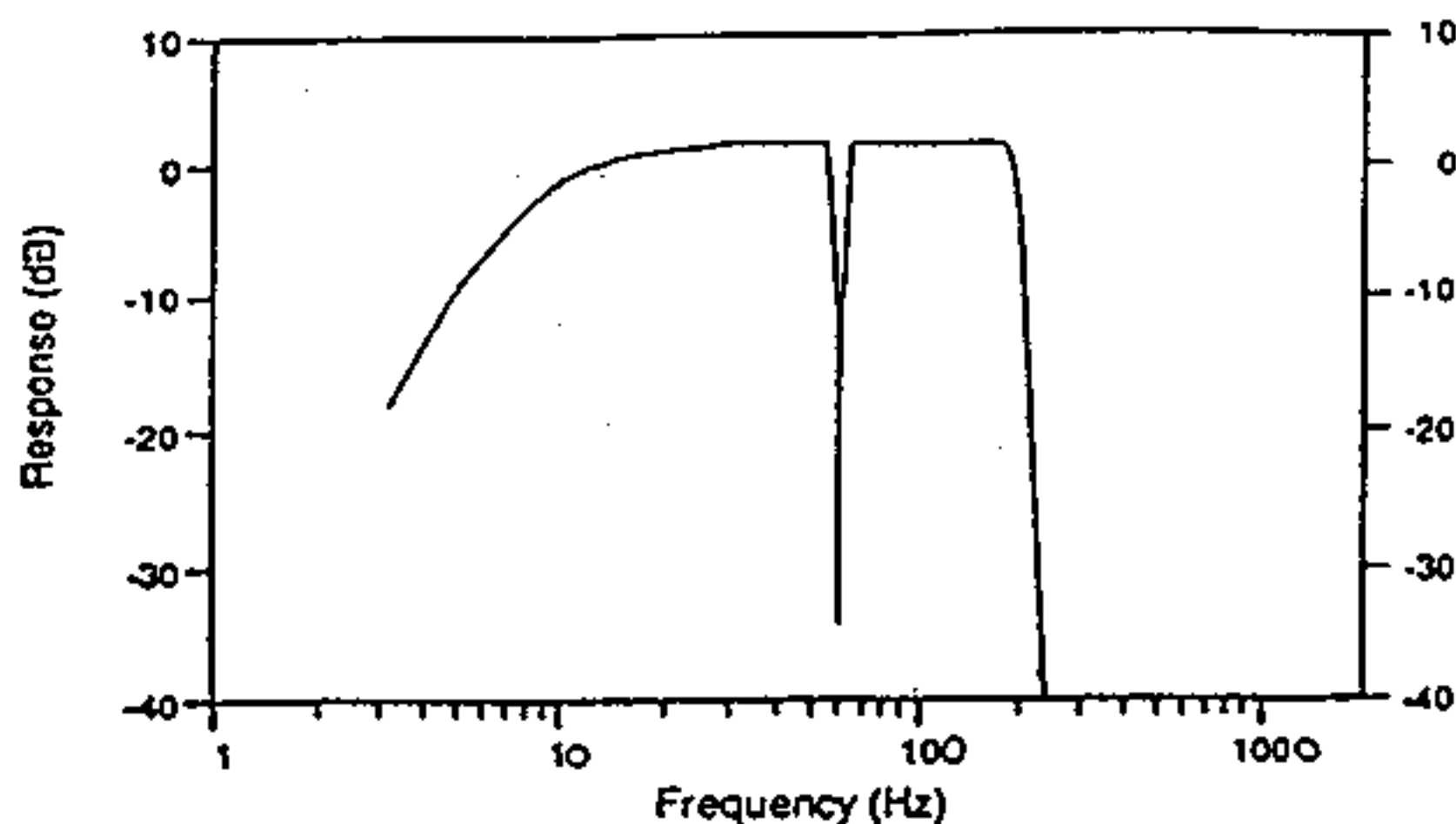


Figure 4: Theoretical instrument response for the SGR

REFTEK

The REFTEK seismographs are three channel, three component instruments owned by IRIS/PASCALL which can be operated in pre-programmed mode or event-detect mode. They were used in pre-programmed mode for this experiment. They can record at a range of sampling rates, and the data recorded in this experiment was sampled at 8 ms. The seismographs were connected to three component Mark Products L-22 2 Hz geophones. The instrument response function is shown in Figure 5 (PASCALL training center manual, unpublished manuscript).

PRS

Two types of PRS were used in the experiment: the PRS-1 and the PRS-4. The PRS-1 is a one component digital instrument with a total dynamic range of 126 dB and a sampling interval of 8.3 ms. The PRS-1 instruments were connected to one component Mark Products L4A 2 Hz vertical geophones. The PRS-4

instruments are similar to the PRS-1 instruments except that they record three orthogonal components. The theoretical instrument response for both PRS -1 and PRS -4 seismographs is shown in Figure 6 (Luetgert et al, 1990).

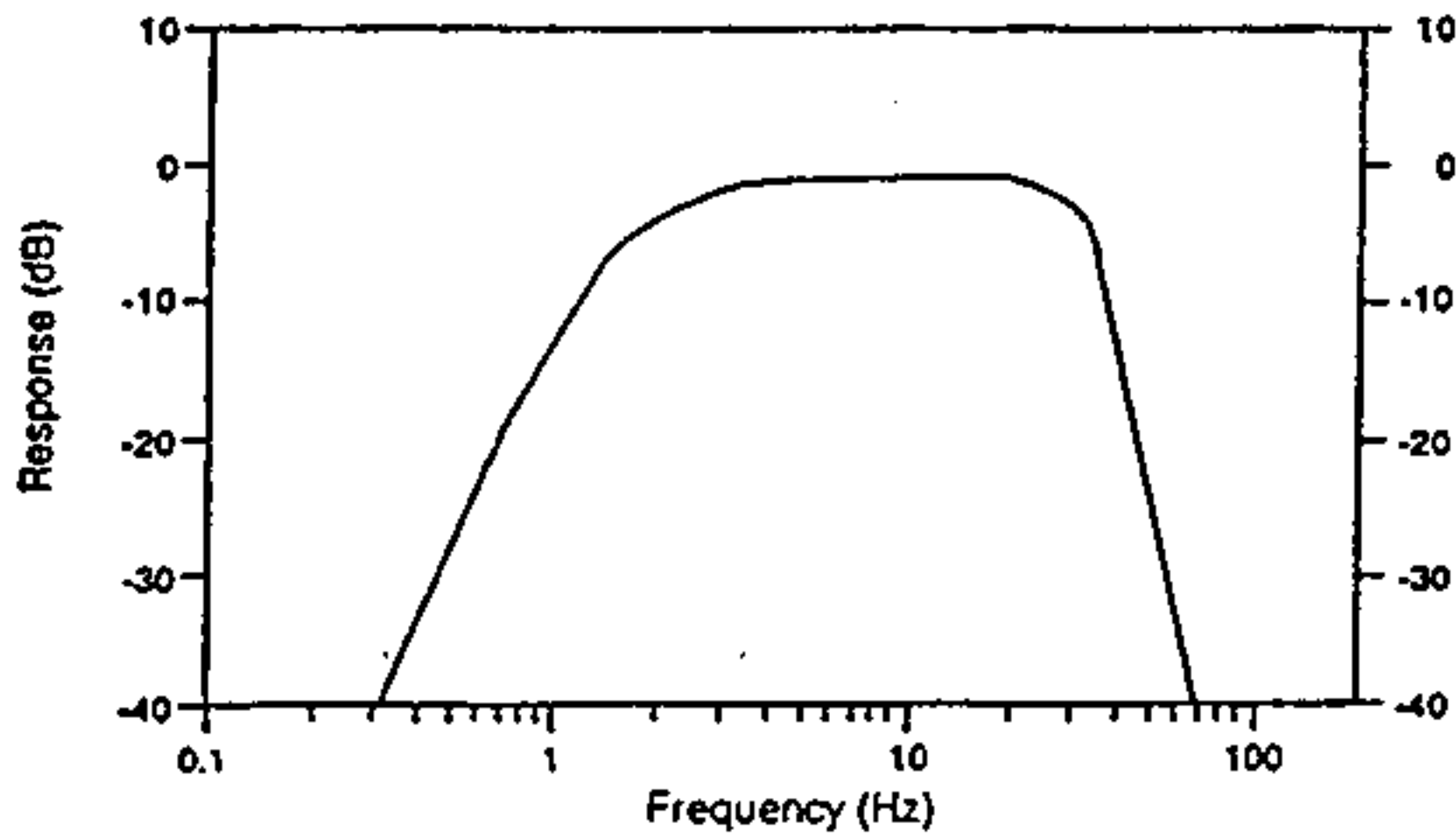


Figure 5: Theoretical instrument response for the REFTEK

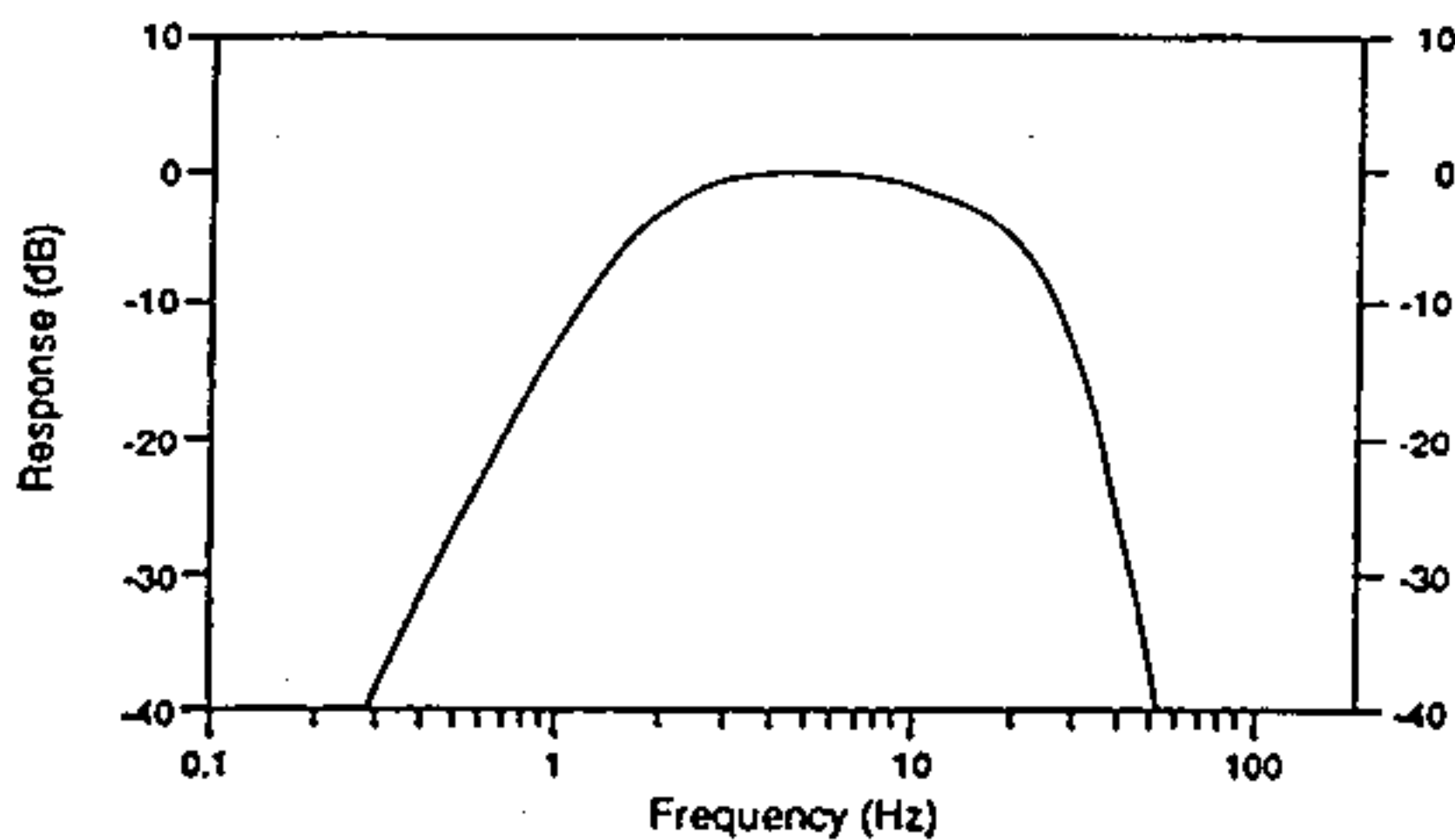


Figure 6: Theoretical instrument response for the PRS

The different instruments were distributed along the lines so that for the most part SGRs and REFTEKS alternated along the lines which means one component instruments alternate with three component instruments allowing coverage of the whole line by three component instruments, and PRS's were put at the eastern end of the two east-west lines (Lines 1 and 6) and at both ends of the north east-south west line (Line 9) since they have a lower frequency response and are more suitable for recording energy out to the longest offsets. The type of instrument located at each station is listed in Tables 2, 3 and 4.

TIMING

Prior to deployment, the internal clocks of each instrument were synchronised with a temperature-compensated master clock which in turn was synchronised

with a satellite clock. The deployed instruments were programmed to begin recording immediately before each shot and to continue recording for 60 seconds before switching off again. When the instruments were picked up after the deployment, the internal clocks were compared to the satellite clock to measure the drift of the internal clocks.

5) COMPARISON OF INSTRUMENT RESPONSES OF COLLOCATED INSTRUMENTS

During the experiment, some sites were instrumented with all three types of seismographs. This was done to compare the response of the different instrument groups during the data analysis phase. There seems to be a different ground motion polarity on the REFTEK instruments. Table 6 shows the locations and channel numbers of the collocated stations, and table 7 shows the channel numbers and locations of instruments placed at shotpoints. Figures 7a to 10b show traces and spectra of collocated instruments, ordered by distance between instrument and shotpoint. They are followed by an example of cultural noise (figure 11a and 11b).

The traces for the comparison of the instrument response were taken directly from the field tapes. Arrivals recorded on SGR and PRS instruments generally line up well. On some of the REFTEKs, however, the first arrivals do not occur at the same apparent time as the arrivals of the other collocated instruments. Although a correction for linear clock-drift was applied (as much as 0.157s for the REFTEK instrument at station 1208), there is still a considerable mismatch left (e.g. figure 9a). This may be, because the total drift on some of the REFTEKs was large and non-linear.

Further data processing steps were debiasing and, in some cases, despiking small offset SGR traces. Despiking was done by manually picking spikes and replacing them with interpolated values. The spikes only occurred in a few SGR traces and at ranges smaller than 35 km. The same instrument showed no spikes for more distant shots. Two three-second windows were selected for the power spectra density plots, one window starting with the first arrival (solid line in the spectra) and the second window for the background noise immediately before the event (dashed line in the spectra). A Bartlett window was applied before the Fourier transform, and a five sample running-average was calculated. Because of the three second window length, the spectra become poorly resolved towards low frequencies.

Towards the high frequency end of the spectrum, an anti-aliasing filter is applied by each instrument. The anti-aliasing filter of the REFTEK instruments is very sharp and the signal level is reduced to background noise level at the Nyquist frequency (figure 7b). This is caused by the different filter technology build in the instrument. REFTEKs record with an instrument-internal, high sampling rate which then is digitally filtered to the sampling rate in the seismogram. In contrast, the SGR and PRS instruments record with the seismogram sampling rate and

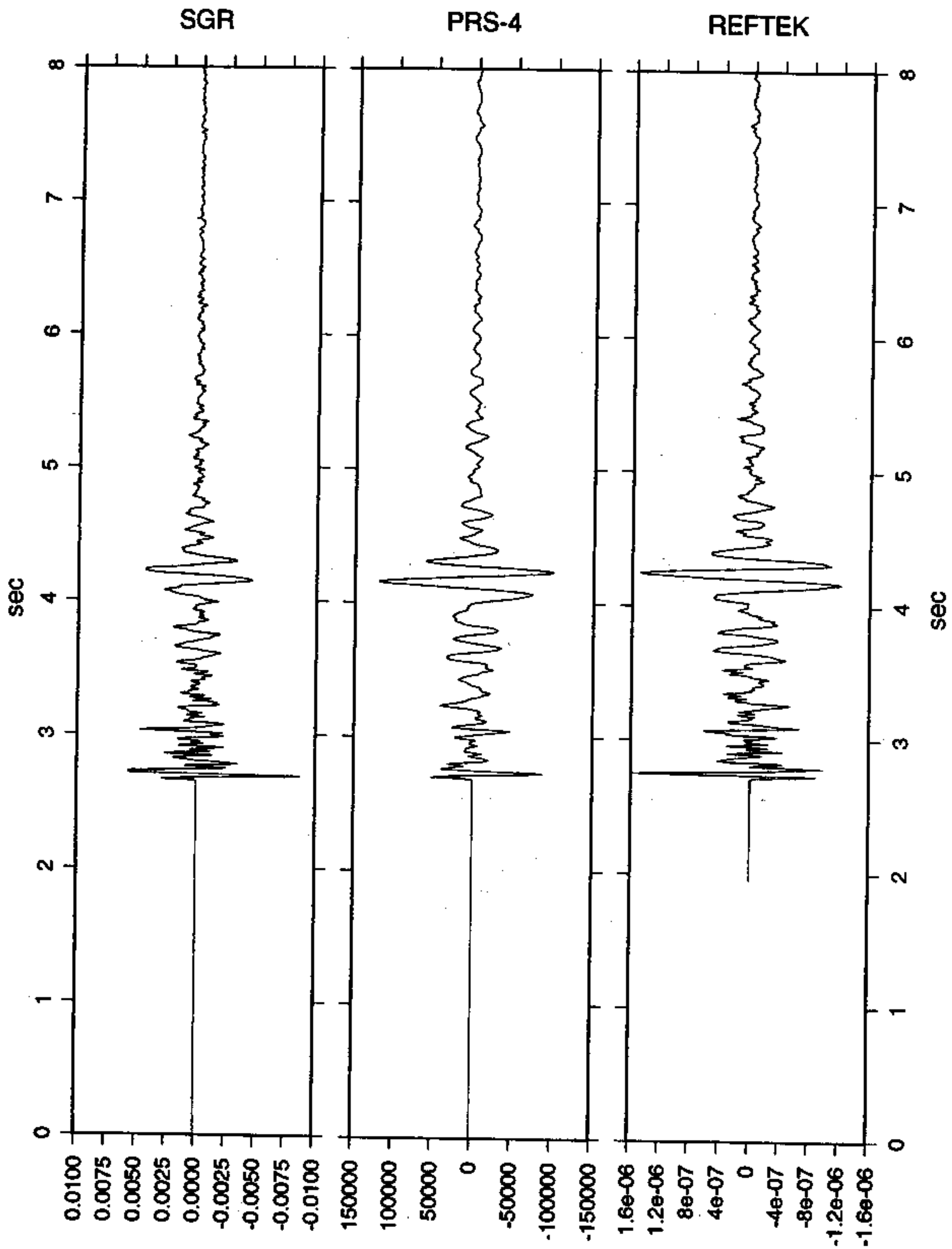


Figure 7a: Traces from collocated station 6208 for shot 603. The range is 2.75 km

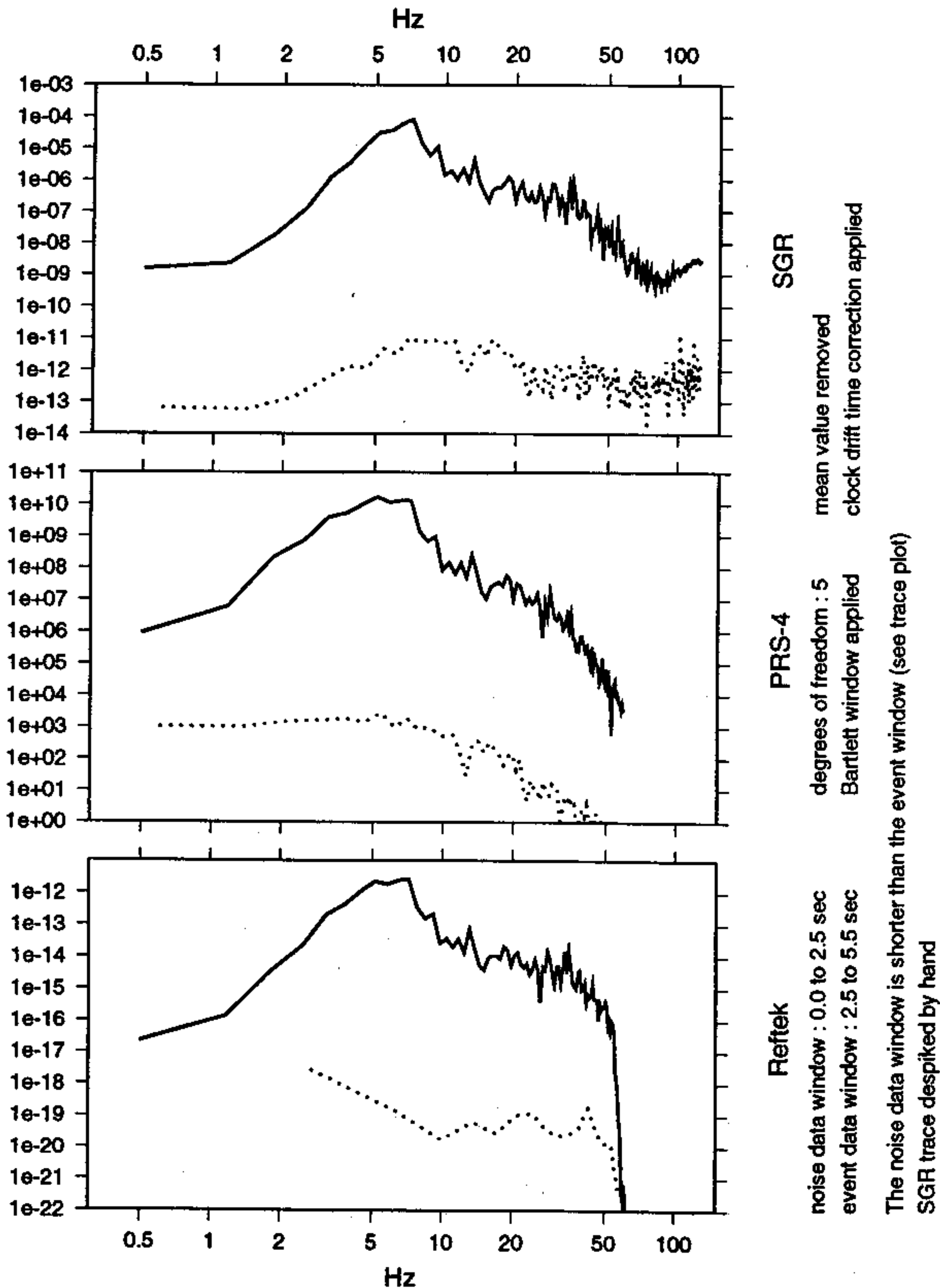


Figure 7b: Spectra from collocated station 6208 for shot 603. The range is 2.75 km

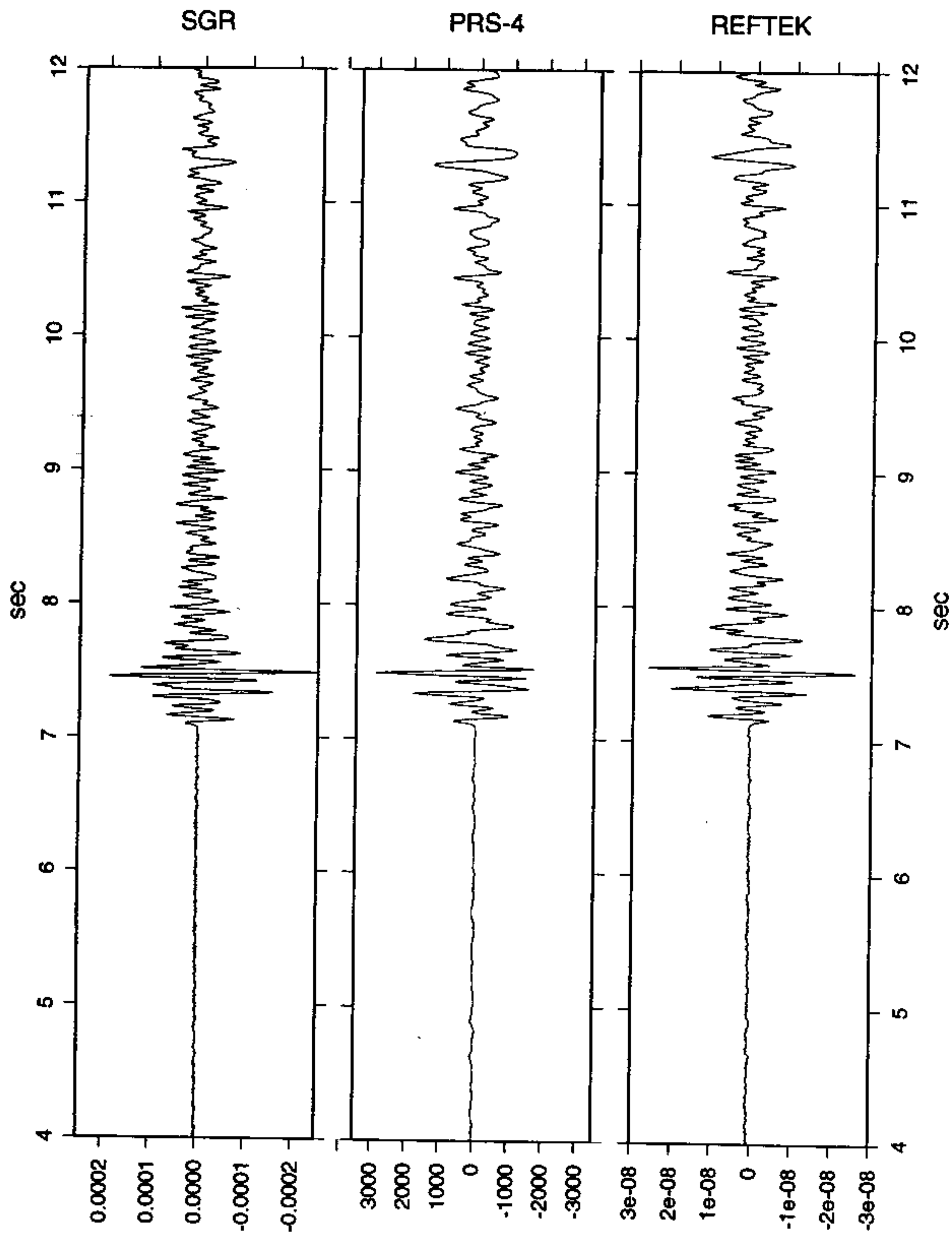


Figure 8a: Traces from collocated station 6208 for shot 604. The range is 28.3 km

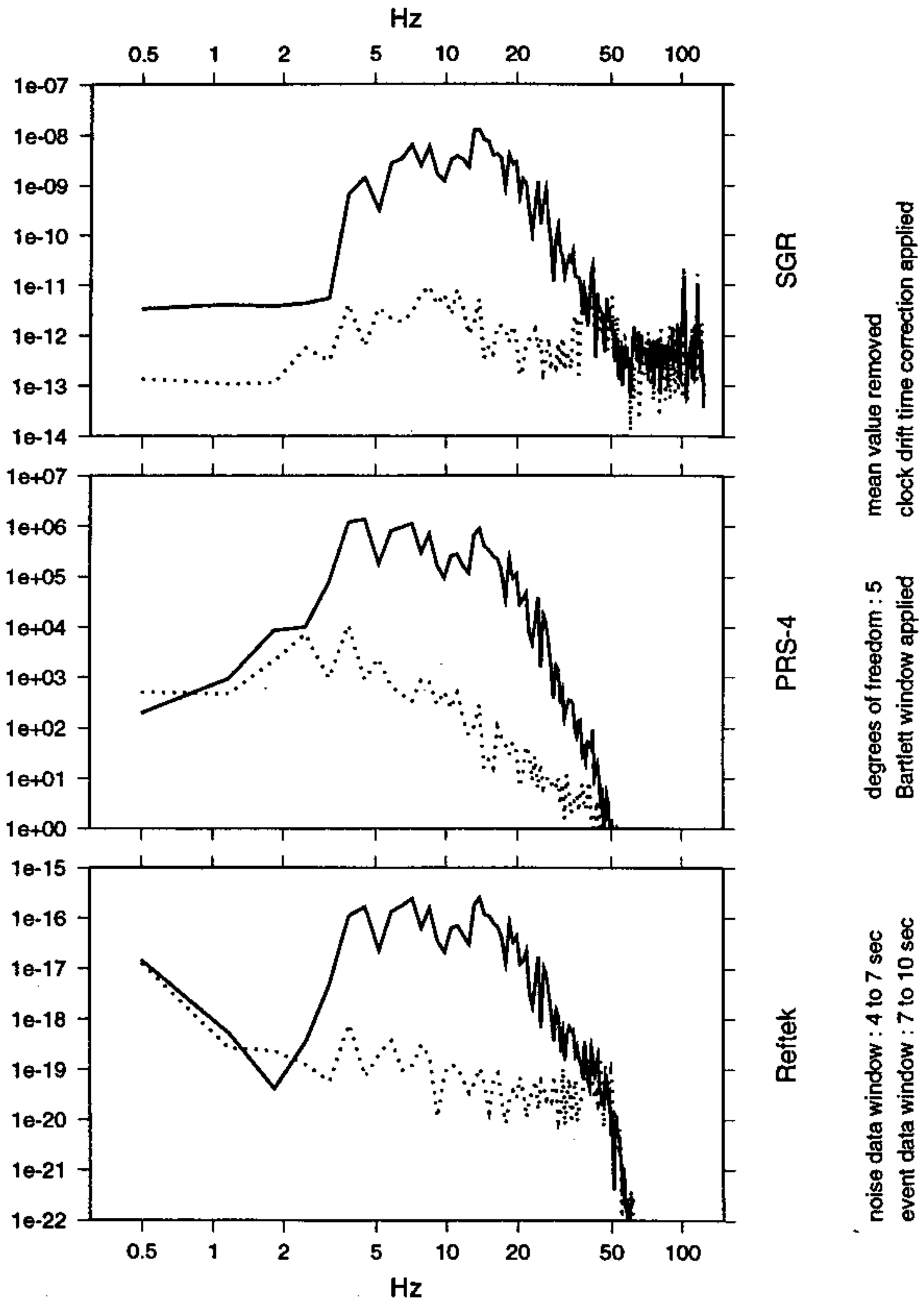


Figure 8b: Spectra from collocated station 6208 for shot 604. The range is 28.3 km

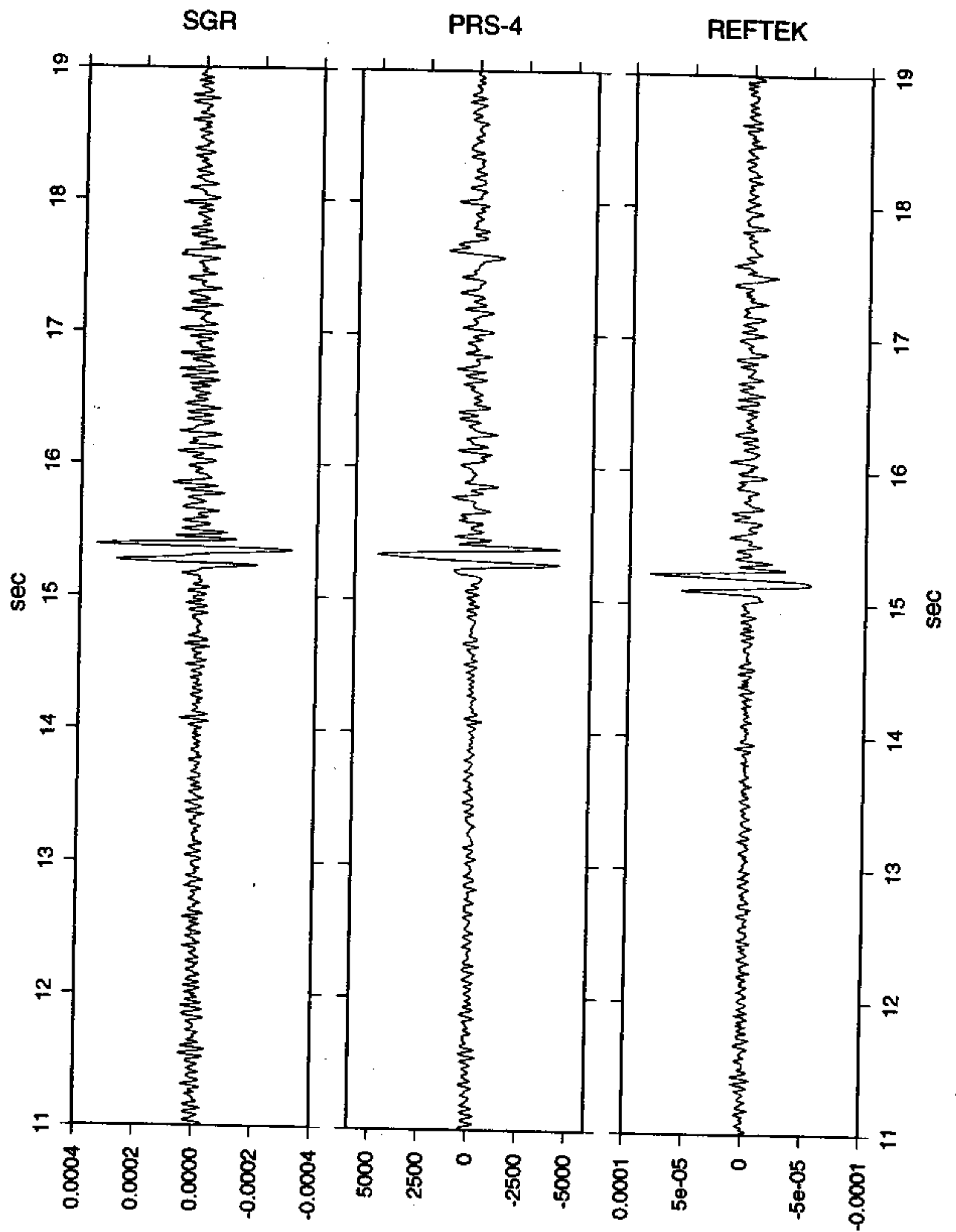


Figure 9a: Traces from collocated station 1208 for shot 101. The range is 73.3 km

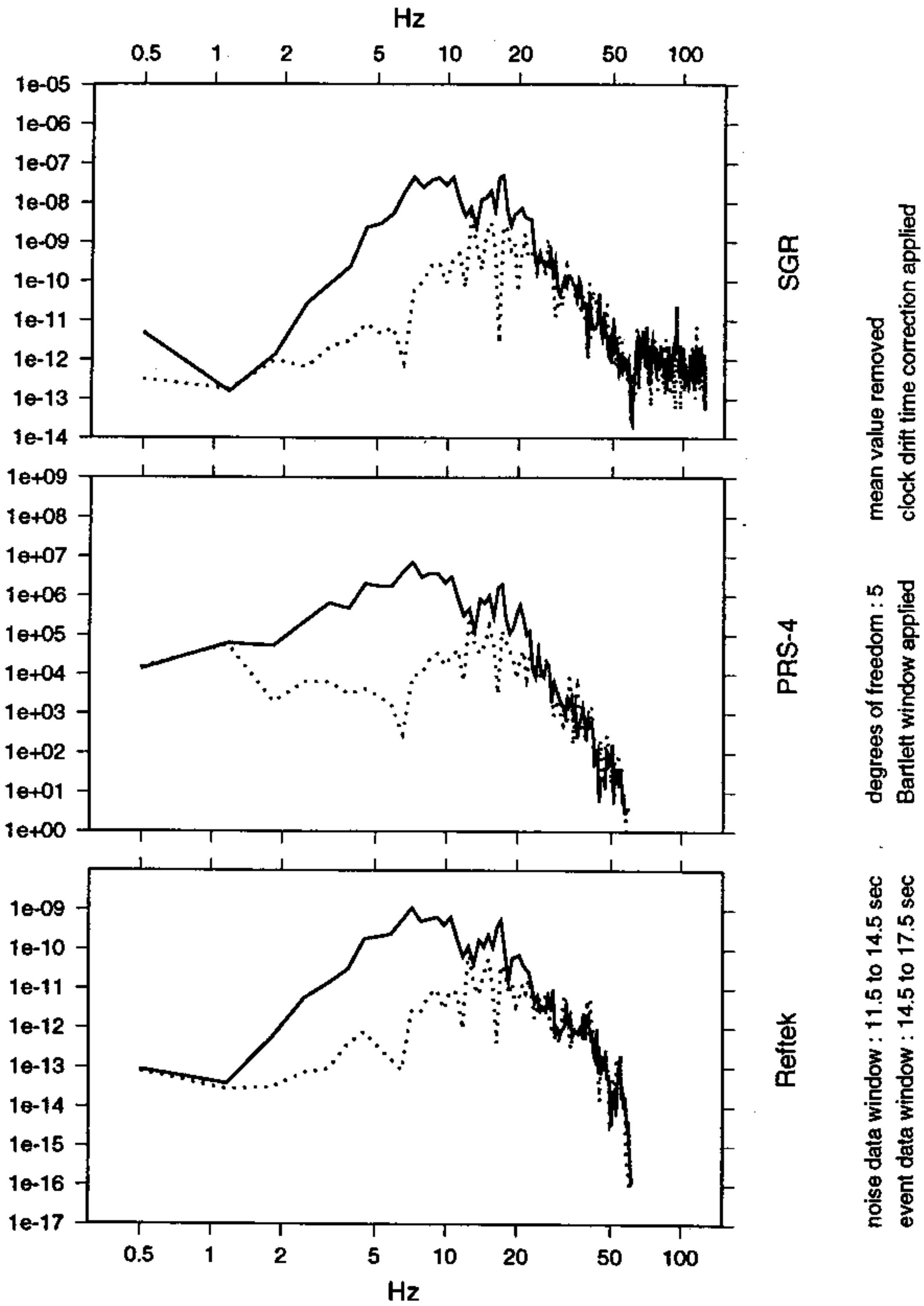


Figure 9b: Spectra from collocated station 1208 for shot 101. The range is 73.3 km

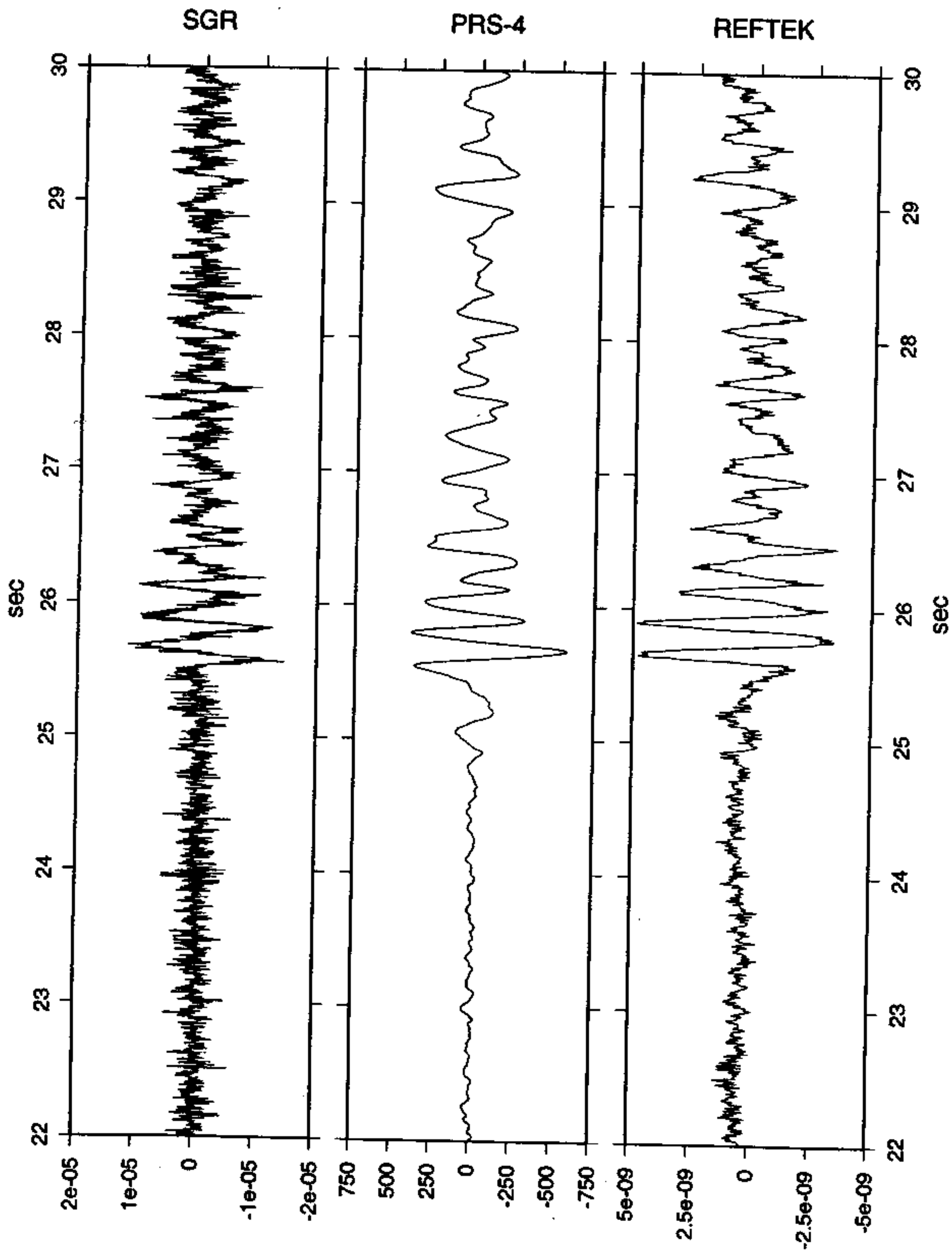


Figure 10a: Traces from collocated station 6208 for shot 608. The range is 125.9 km

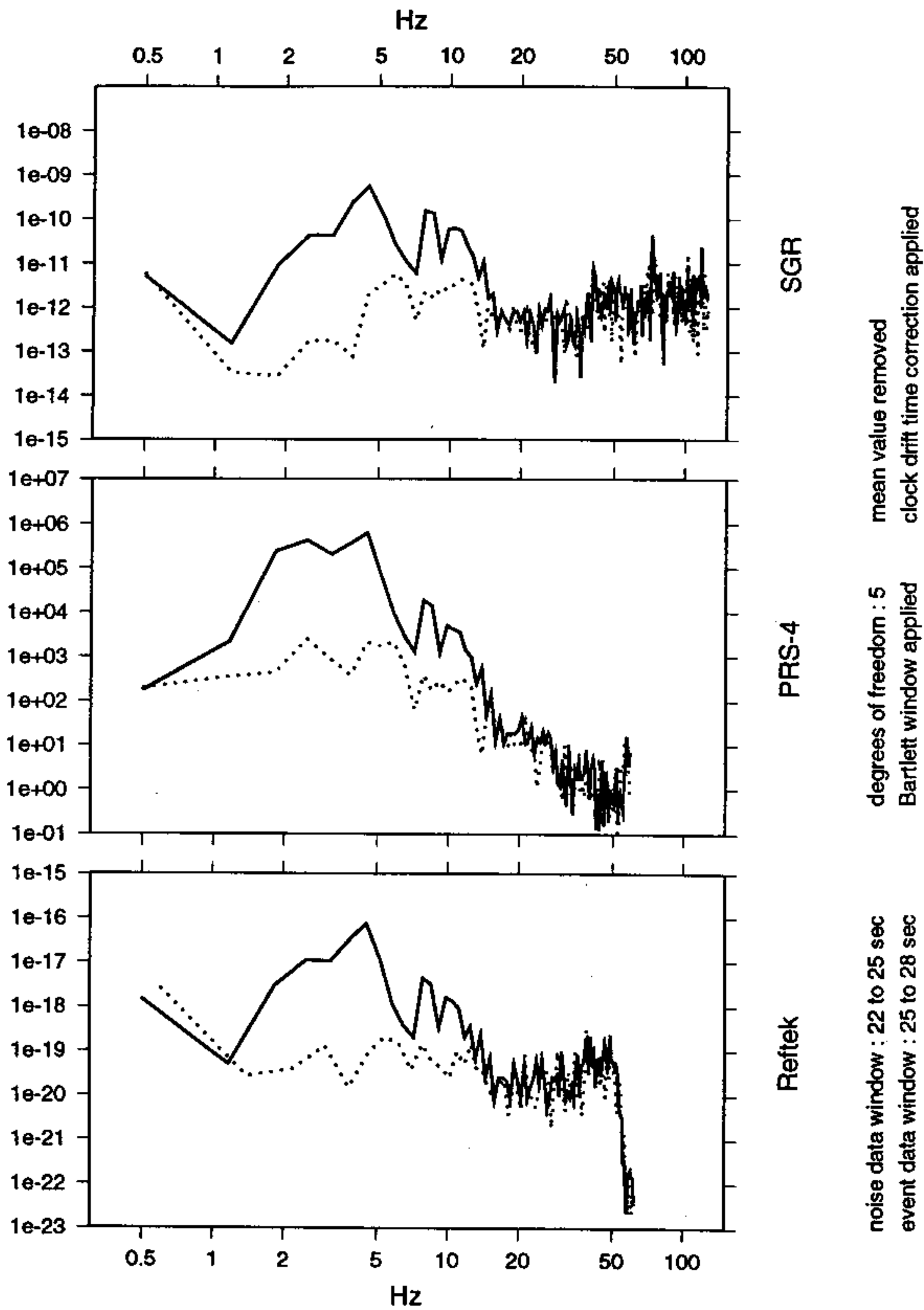


Figure 10b: Spectra from collocated station 6208 for shot 608. The range is 125.9 km

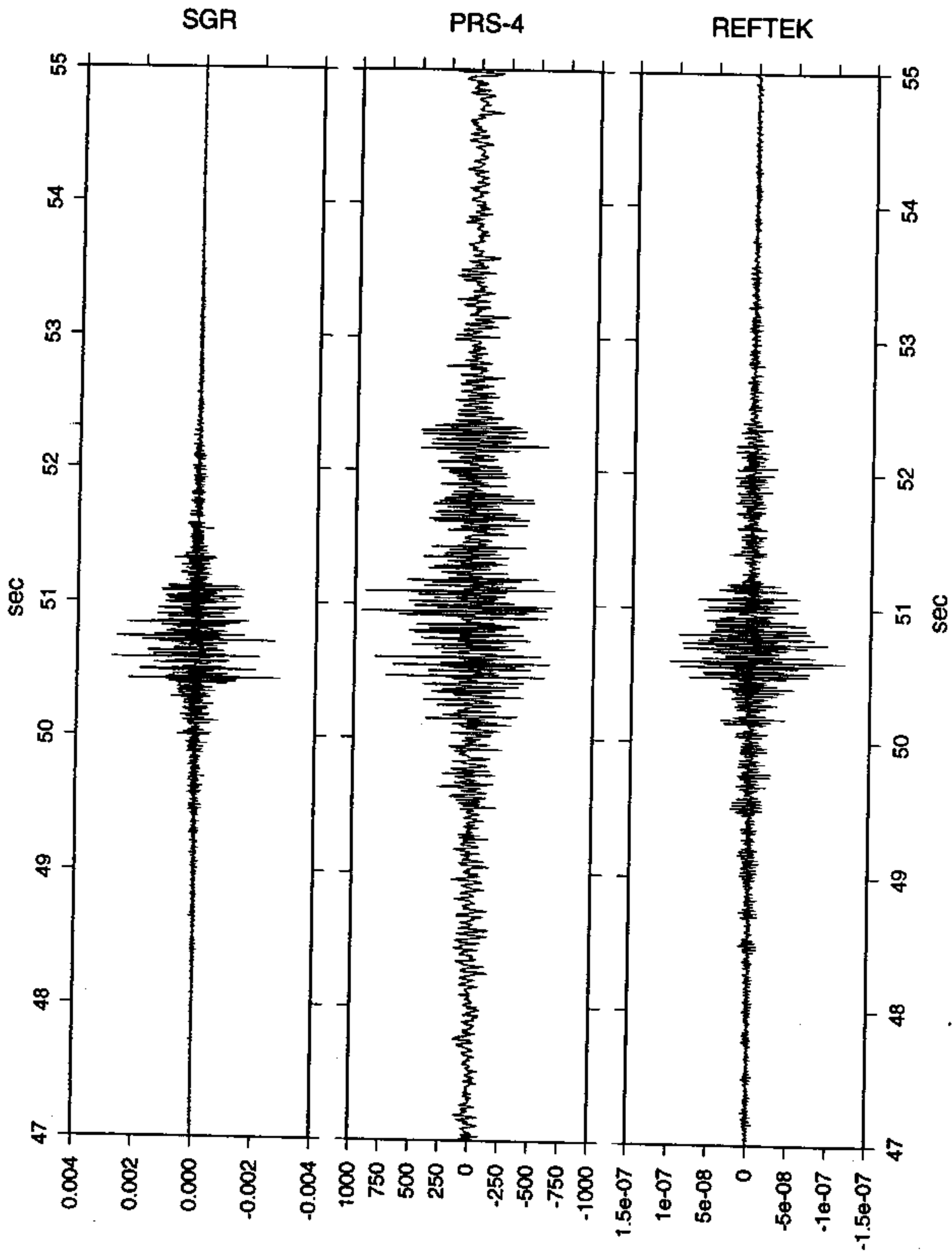


Figure 11a:Traces from collocated station 6208 for shot 606. The range is 78.6 km

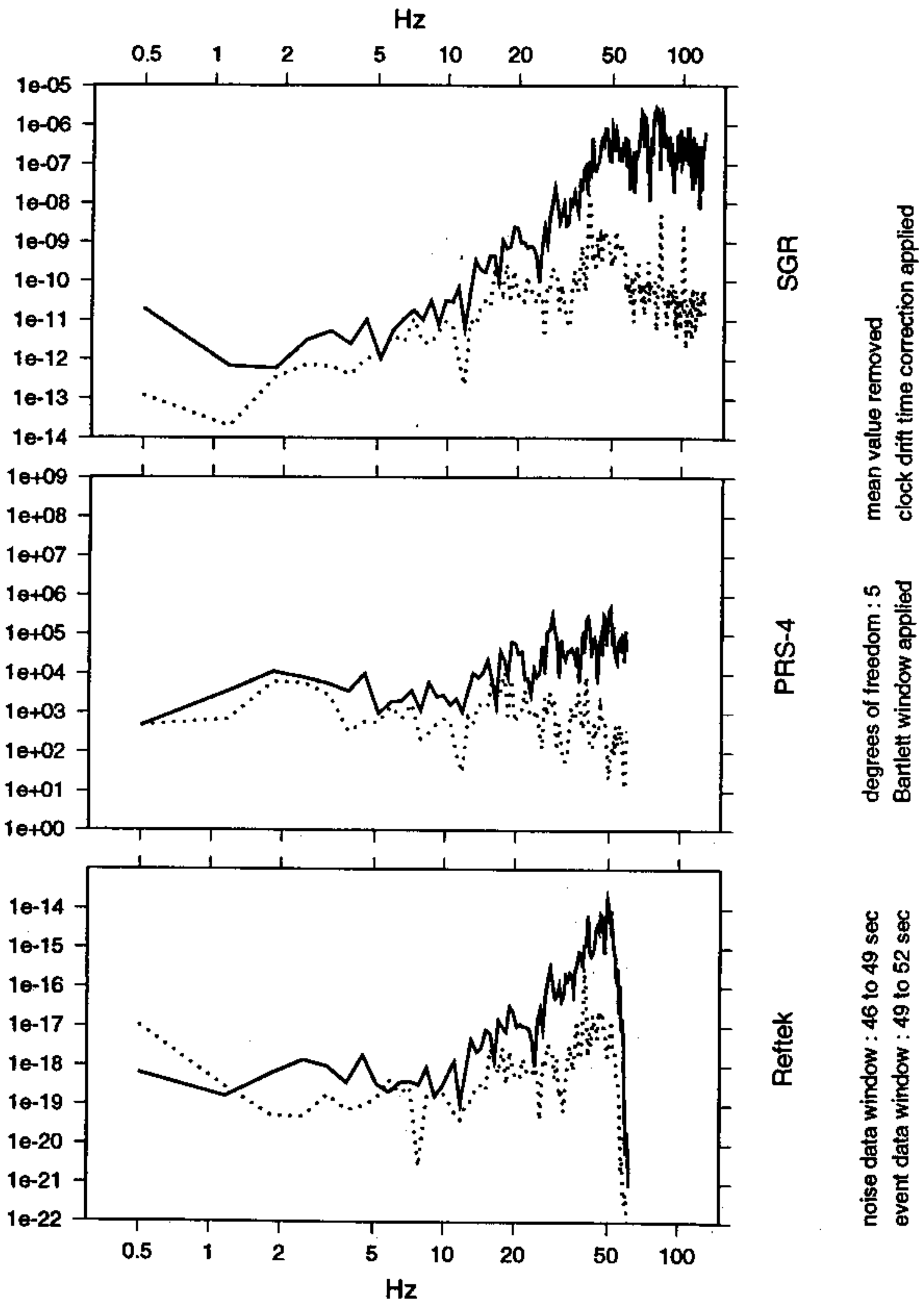


Figure 11b: Spectra from collocated station 6208 for shot 606. The range is 78.6 km

apply an analog anti-aliasing filter. The PRS instruments have a less steep anti-aliasing filter. A typical spectrum is shown in figure 8b.

There is a significant slope in the background noise spectrum, while for the same station and shot, REFTEK and SGR instruments show almost horizontal background noise spectra. The SGR instruments have such a high Nyquist frequency (125 Hz) that the anti-aliasing filter only becomes important for very short ranges (figure 7b) and for strong cultural noise containing frequencies near the Nyquist frequency (figure 11b). For those cases only, the PRS and the SGR anti-aliasing filter both fail to attenuate strong high frequency signals, causing a potential aliasing problem. No investigation of phase shifts caused by the anti-aliasing filters was done.

For large shot-receiver ranges, the spectrum of the signal shifts towards lower frequencies (compare figures 7b, 8b, 9b and 10b). The quality of the recordings at low frequencies depends mostly on the seismograph used by the instrument. It is not surprising that the PRS instrument performs the best, since it is the only instrument with a 2 Hz seismograph. Figure 10a nicely shows the dominating long periods in the signal. The PRS trace is the smoothest trace since high frequency background noise is attenuated by the shallow slope of the PRS anti-aliasing filter. Although the seismic profile is about 200 km long, the largest useful offset for collocated instruments is 125.9 km, shown in figure 10a and 10b. Only shot 108 for trace 1126 would give a larger distance (156 km). Unfortunately the signal was too attenuated to be of any use. The full range of 200 km is not reached since collocated instruments were not deployed at the ends of the line.

6) DATA REDUCTION

Data from the different instruments were reduced as outlined below and then the datasets were merged into nine SEG-Y format files, one for the vertical component data for each line, one for the horizontal component data (both north-south and east-west components) for each line and one for the collocated stations for each line. The first six SEG-Y files include geometry, but the last three SEG-Y files (for the collocated instruments) do not include geometry. The locations for the stations in these files are given in Table 6 and 7. All the SEG-Y header positions are listed in Table 5.

SGR

The following processing was done:

- resampled from 4 ms to 8 ms using a 60 Hz anti-alias filter.
- corrections made for offset dependent start times
- clock drift static applied
- DC offset removed

REFTEK

- DC offset removed
- the three component data was split up and the vertical component data was put in one SEG-Y file and the horizontal components were put in another SEG-Y file

- polarity reversed to bring into line with the data recorded on the SGRs and PRSs
- clock drift static shift applied

PRS

The data from the Canadian Geological Survey was distributed as a SEG Y disk image and was then processed as outlined below:

- resampled from 8.33 to 8 ms using a 60 Hz anti-alias filter
- DC offset was removed from the data
- the three component data (PRS-4s) was split up and the vertical component data was put in one SEG Y file and the horizontal components were put in another SEG Y file
- clock drift static shift applied

The three datasets recorded on the different instruments were then merged and sorted by shotpoint number (= Field File Identification number (FFID)) and channel number. The geometry (calculated using Green Mountain Geophysics Inc. crooked-line-geometry software) was then added to the merged file using the shot and receiver locations shown in Tables 1 through 4. Offsets for stations to the east for lines 1 and 6 and to the south for Line 9 are defined as having negative offset. Shotpoints 606 and 607 were set off by a wrist watch and are 3-4 s late. This has not been altered in the data on the tapes. The correct static to apply to bring these shot times back to a zero start time is 3750 ms back towards zero for shotpoint 606 and 2950 ms back towards zero for shotpoint 607.

The final merged SEG Y files sampled at 8 ms, with trace lengths of 60 s can be obtained from

Jim Fowler,
I.R.I.S.,
1616 N. Ft. Myer Dr.,
Suite 1050,
Rosslyn, VA 22209

7) RECORD SECTIONS

Shot gathers of all the vertical component data and select horizontal component data are shown in this section. The horizontal data was generally of poor quality with very low signal to noise and with small ranges of energy propagation laterally. The best example from each line is shown here (shotpoints 104, 605 and 906).

All sections are displayed as trace normalized plots with a reduction velocity of 6 km/s for the vertical component data and 3.46 km/s for horizontal component data, such that the reduced time shown on the time axis of the plots is given by

$$T_R = T - x/6 \text{ (vertical components)}$$

or

$$T_R = T - x/3.46 \text{ (horizontal components)}$$

where x is the offset in km and T is the unreduced time in seconds. A 2 -16 Hz bandpass filter was applied to the data. No elevation statics have been applied although the elevation plots shown in Figure 3 show that there is a large variation in elevation across each line.

Shotpoints 606 and 607 were set off by a wrist watch and are 3-4 s late. The plots shown in this section have had a static shift applied to them to bring the shot times back to zero start time. Shotpoint 606 has had a -3750 ms shift applied to it and shotpoint 607 has had a - 2950 ms shift applied to it. Shotpoint 102 does not start at zero because it was about 1 km off the line of receivers, in an orchard which was probably underlain by lower velocity sediment than the material underlying the closest receivers.

Sections are vertical component sections unless they are marked as north-south or east-west component sections.